Magnetite (Fe_3O_4): a new variant of relaxor multiferroic?

2012 J. Phys.: Condens. Matter 24 086007

(http://iopscience.iop.org/0953-8984/24/8/086007)

J. Phys.: Condens. Matter **24** (2012) 086007 (8pp) doi:10.1088/0953-8984/24/8/086007

Magnetite (Fe_3O_4): a new variant of relaxor multiferroic?

M Ziese[1], P D Esquinazi[1], D Pantel[2], M Alexe[2], N M Nemes[3] and M Garcia-Hernández[4]

[1] Division of Superconductivity and Magnetism, Faculty of Physics and Geosciences, University of Leipzig, D-04103 Leipzig, Germany
[2] Max Planck Institute of Microstructure Physics, D-06120 Halle, Germany
[3] GFMC Departamento Física Aplicada III, Universidad Complutense de Madrid, E-28040 Madrid, Spain
[4] Instituto de Ciencia de Materiales de Madrid-CSIC, Cantoblanco, E-28049 Madrid, Spain

E-mail: ziese@physik.uni-leipzig.de

Received 18 November 2011, in final form 5 January 2012
Published 8 February 2012
Online at stacks.iop.org/JPhysCM/24/086007

Abstract
The electric polarization, dielectric permittivity, magnetoelectric effect, heat capacity, magnetization and ac susceptibility of magnetite films and polycrystals were investigated. The electric polarization of magnetite films with saturation values between 4 and 8 μC cm^{-2} was found to vanish between 32 and 38 K, but in polycrystals no phase transition was detected in this range by heat capacity. Both types of samples showed magnetoelectric effects at low temperatures below a frequency-dependent crossover. This is interpreted as arising from multiferroic relaxor behavior.

(Some figures may appear in colour only in the online journal)

1. Introduction

Magnetite (Fe_3O_4) is an archetypical magnetic material. It crystallizes in the inverse spinel structure with Fe^{3+} ions occupying the tetrahedrally coordinated A sites and both Fe^{2+} and Fe^{3+} ions sharing the octahedral B sites. Exchange interactions between the iron sites are antiferromagnetic with A–B sublattice exchange being dominant. This leads to ferrimagnetic ordering with a magnetic moment per formula unit close to 4 μ_B and a high Curie temperature of 860 K. Magnetite undergoes an electronic and structural transition at about 120 K—the Verwey transition—into a charge-ordered phase [1].

The charge-ordering pattern as well as the symmetry of the low temperature phase are still a matter of debate, see, e.g., [2–7], but it is clear that only the arrangement of the Fe^{2+} and Fe^{3+} ions on the B sites is relevant for the charge-ordering pattern. The B sites themselves form a pyrochlore lattice consisting of corner-sharing tetrahedra [8]. Anderson suggested that each tetrahedron is occupied by two Fe^{2+} and two Fe^{3+} ions (the Anderson rule) to maximize the number of Fe^{2+}/Fe^{3+} pairs [8]. First studies of the crystalline symmetry pointed towards an orthorhombic $\sqrt{2} \times \sqrt{2} \times 2$ cell [9–11] with the c axis along one of the original cubic directions, e.g. [001], and the a and b axes along the cubic [1$\bar{1}$0] and [110] directions, respectively. More recent structural studies found a monoclinic structure [12] either with space group [13, 14] $P2/c$ or with space group [2, 6, 15] Cc. Recent theoretical studies using density functional theory were based on these structure determinations [16–19] and found a violation of the Anderson rule. Moreover, a comparative density functional theory study of four possible low temperature structures for magnetite revealed the Cc structure to be the ground state structure. In this structure 1/4 of the tetrahedra satisfy the Anderson rule with a 2:2 Fe^{2+}/Fe^{3+} occupation, but 3/4 of the tetrahedra violate the Anderson rule with a 3:1 either Fe^{2+}/Fe^{3+} or Fe^{3+}/Fe^{2+} occupation.

It has long been known that magnetite shows magnetoelectric effects in its low temperature phase [20–33]. This has important implications not only on the multiferroic nature of magnetite, but also on the structural symmetry that was deduced to be triclinic [30]. Although there are indications for triclinic symmetry from structural studies [12], a clear

confirmation is still absent. Firm proof for the existence of ferroelectric order in magnetite films has only been presented recently [34], making magnetite an archetypical multiferroic material. The appearance of ferroelectric order below about 38 K has been explained by the existence of a spontaneous electric polarization in the non-centrosymmetric monoclinic *Cc* structure arising from an alternation of charge states and bond lengths [35, 36]. It is surprising, however, that the electric polarization does not already develop at the Verwey transition, when magnetite enters the monoclinic phase, since the *Cc* structure was found to be present between 4 K and T_V [2].

The aim of this work is the study of the magnetic, electric and magnetoelectric properties mainly of magnetite films. The emphasis was put on films for two reasons. Firstly, the film–substrate strain leads to a preferential orientation of the *c* axis [37], thus eliminating certain twin orientations and simplifying the microstructure. Secondly, in view of potential applications of multiferroics, e.g. in tunneling junctions and memory devices, the understanding of the magnetoelectric coupling in thin films is of prime importance. We focus especially on the detection of a possible phase transition around 40 K pertaining to the ferroelectric phase.

2. Experimental details

Magnetite films of 150 nm thickness were grown on Nb-doped $SrTiO_3$ (001) substrates by both pulsed laser deposition (PLD) and RF magnetron sputtering. For the PLD process a KrF excimer laser (Lambda Physik model LPX300) operating at a wavelength of 248 nm (KrF), a repetition rate of 10 Hz and a pulse energy of 600 mJ was used. The substrate temperature was 430 °C and the oxygen partial pressure during deposition 9×10^{-6} mbar. After film deposition the oxygen flow was immediately stopped, the chamber was quickly evacuated below 10^{-7} mbar to avoid oxidation of the magnetite film and the sample was rapidly cooled. The films were ferrimagnetic with Verwey temperatures of 115 K (PLD films) and 117 K (sputtered films), respectively.

X-ray diffraction measurements at room temperature were performed with Cu Kα radiation using a high resolution Philips X'pert diffractometer. θ–2θ scans only showed (00*l*) reflexes indicating epitaxial growth. The out-of-plane lattice constant of the films was determined as 0.846 nm, somewhat larger than the bulk value of 0.8397 nm. This is consistent with the considerable compressive stress exerted by the $SrTiO_3$ substrate that has a lattice constant of 0.3905 nm. Transmission electron microscopy showed a grain size of about 100 nm [34]. For comparison a polycrystalline magnetite sample was prepared by a standard solid state reaction technique. The Verwey temperature of the sample was 123 K.

For measurements of the ferroelectric polarization Pd top metal electrodes (with an area of 60×60 μm^2) were deposited by thermal evaporation through a shadow mask. Ferroelectric hysteresis loops were measured with a Ferroelectric Analyzer (TF2000, aixACCT). PUND (positive up, negative down) pulse measurements were performed by applying 100 ns–5 μs wide pulses of variable voltage using a pulse generator (Tektronix AFG3102) and measuring the signal generated by the current on a 50 Ω load resistance with an oscilloscope (Tektronix TDS684C). The ac impedance $Z = Z' + iZ''$ was measured by a Hewlett Packard impedance analyzer (HP4194A). Magnetocapacitance measurements were performed in an Oxford Instruments cryostat equipped with a 9 T superconducting solenoid using an Andeen-Hagerling AH2500 capacitance bridge operating at a fixed frequency of 1 kHz. In both cases the dielectric permittivity was calculated from the admittance Z^{-1} by $\epsilon = Z^{-1}/i\omega C_G$, where i denotes the imaginary unit, ω the angular frequency and $C_G = \epsilon_0 A/d$ the geometrical capacitance of an equivalent capacitor with the sample geometry (area A and thickness d). ϵ_0 denotes the vacuum permittivity. Magnetic fields were applied parallel and perpendicular to the magnetite film, while the electric field was applied along the surface normal. Magnetization measurements were performed with a SQUID magnetometer (Quantum Design, model MPMS-7). AC susceptibility measurements were performed in an ac susceptometer (Lakeshore, model 7000) using a sample holder providing electrical contacts to the sample.

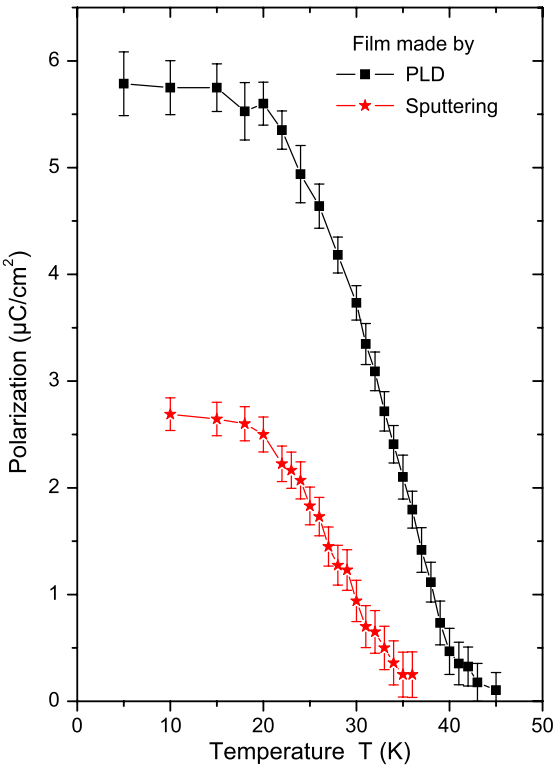

Figure 1. Electric saturation polarization of the magnetite films made by pulsed laser deposition and magnetron sputtering.

3. Results

3.1. Electric polarization of magnetite films

Figure 1 shows the measured saturation polarization of PLD and sputtered films as a function of temperature. The electric polarization saturates at low temperatures at about

5.8 μC cm^{-2} (PLD film) and 2.7 μC cm^{-2} (sputtered film), respectively. At higher temperatures the temperature dependence is approximately quadratic, extrapolating to zero at 38 and 32 K. The electric polarization of a magnetite single crystal was determined as $\vec{P} = (4.8, 0, 1.5)$ μC cm^{-2} [27]; the components of the polarization vector refer to the monoclinic axes.

Theoretically an electric polarization with a vanishing component along the *b* axis was predicted [34, 36]. Depending on the theoretical approach used for the calculation (Berry phase, point charge model, dipole moments), for the other two polarization components values of $P_a = 4.0$–4.4 μC cm^{-2} and $P_c = 4.1$–5.7 μC cm^{-2} were obtained.

A comparison of the experimental and theoretical values is not straightforward, since the samples might have an intricate domain and twin structure. Here we briefly discuss literature data and then our own results. Effects of the twin structure were analyzed in detail by Miyamoto and Chikazumi [30] and it was shown that the absolute value of the magnetoelectric effect was strongly dependent on the actual twin structure. The *c*-axis orientation in the low temperature phase of magnetite can be determined by certain cooling procedures through the Verwey transition in applied magnetic fields [9, 38, 37, 39, 40]. Moreover, the application of stress along a cubic ⟨100⟩ direction leads to a preferential orientation of the *c* axis along this direction [9]. The preparation of a twin-free magnetite single crystal in the low temperature phase requires a combination of magnetic field and stress cooling [30], and it is not obvious that this procedure was applied to the sample studied by Kato *et al* [27]. Therefore the polarization values specified in [27] can only be regarded as lower limits. In the case of the magnetite films discussed here the electric polarization was measured after zero-field cooling, such that domain formation was only influenced by the stress exerted by the substrate onto the film. It is known that magnetite films grown on MgO are under slight tensile in-plane stress that leads to a preferential orientation of the *c* axis along the substrate normal [37]. The films studied here are under compressive in-plane stress; therefore the *c* axis is expected to be in-plane, whereas the *a* and *b* axes make angles of about 45° with the substrate normal. Assuming that a single crystallographic domain exists under the metal top electrode, in the experiment the projection of P_a onto the substrate normal is measured, such that $P_a = 8.2$ μC cm^{-2} (PLD film) and $P_a = 3.8$ μC cm^{-2} (sputtered film) are obtained. The difference in the polarization values of the sputtered and PLD films, however, shows that the assumption of a single crystallographic domain is unlikely to be fulfilled. We speculate that the differences in the polarization values are caused by differences in the actual crystallographic domain and twin structure. At present we can only conclude that experimental and theoretical polarization values are of the same order of magnitude.

3.2. Dielectric permittivity of magnetite films

The real ϵ' and imaginary ϵ'' part of the dielectric permittivity of a PLD-fabricated magnetite film are shown in figure 2(a). The measurements were made in zero magnetic field for various frequencies. Both permittivity components shown in figure 2(a) indicate a strongly frequency-dependent relaxation process between 20 and 50 K. In comparison with conventional ferroelectrics, which show frequency-independent maxima in both permittivity components at the Curie temperature, the dielectric response of the magnetite film does not indicate a phase transition, but a dynamical process. The features in the dielectric permittivity occur in the temperature region, in which the electric polarization decreases from a low temperature saturation value to zero. The strong frequency dependence, however, is characteristic of either a relaxor ferroelectric [41] or of the Maxwell–Wagner effect [42, 43]. There are two arguments against Maxwell–Wagner behavior: (i) similar intrinsic relaxation processes were also observed in the dielectric permittivity of magnetite single crystals [44–46] and (ii) the magnetoelectric effect in magnetite polycrystals is frequency-independent, see section 3.3. Therefore we discard an interpretation of the dielectric measurements within the Maxwell–Wagner model, but regard it as indicative of ferroelectric relaxor behavior.

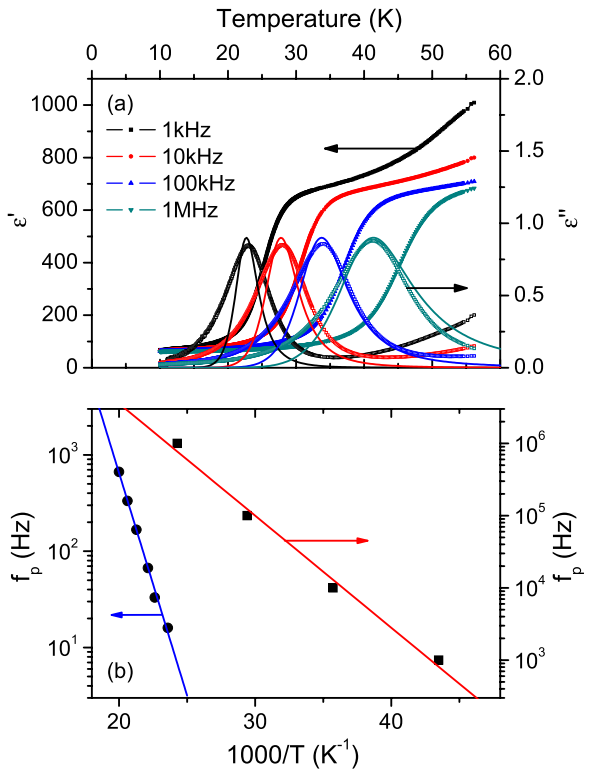

Figure 2. (a) Real ϵ' (left scale) and imaginary ϵ'' (right scale) part of the dielectric permittivity of the magnetite film in zero magnetic field for various frequencies. The solid lines are a fit of a Debye process to the data. (b) Right scale: Arrhenius plot of the dielectric loss maxima. Left scale: Arrhenius plot of the ac susceptibility loss maxima of the magnetite polycrystal, see also figure 6.

In typical relaxor ferroelectrics not only the temperature of the ϵ'' peak is frequency-dependent, but also the height of the maximum decreases with increasing frequency [41]. The data on the magnetite film in figure 2 are clearly

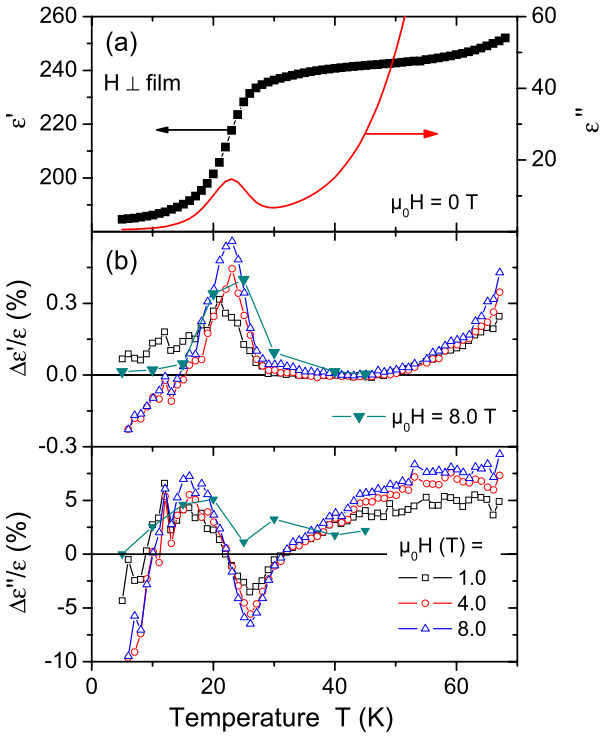

Figure 3. (a) Real ϵ' (left scale) and imaginary ϵ'' (right scale) part of the dielectric permittivity of a magnetite film in zero magnetic field for a frequency of 1 kHz. Relative change of the (b) real $\Delta\epsilon'/\epsilon'$ and (c) imaginary $\Delta\epsilon''/\epsilon''$ part of the dielectric permittivity measured in various magnetic fields. The open symbols were obtained by sweeping the temperature in a constant magnetic field applied at 5 K; the solid symbols represent data obtained from hysteresis measurements at constant temperature.

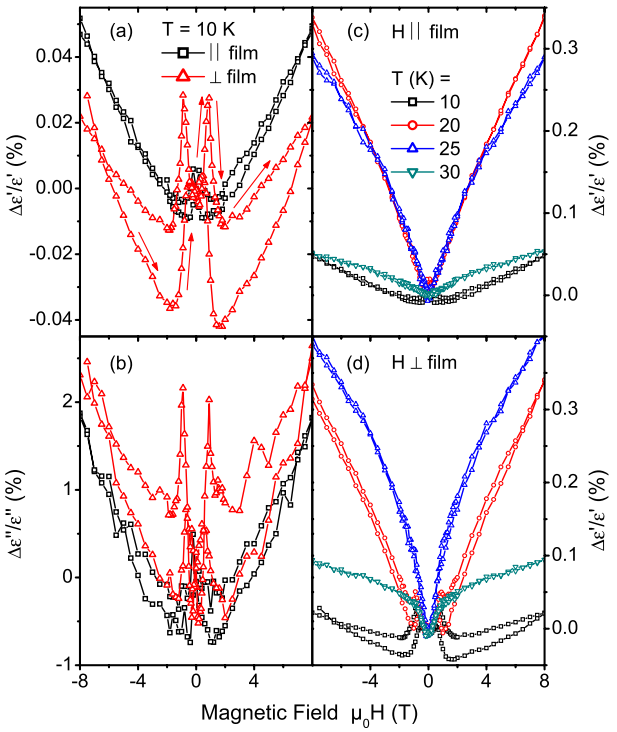

Figure 4. Magnetic field dependence of the (a) real and (b) imaginary parts of the dielectric permittivity at 10 K. Magnetic fields were applied either in-plane or perpendicular to the film. (c) and (d) show corresponding data of the real part of the permittivity at various temperatures.

different from that and are more reminiscent of a Debye process [47]. However, studies of dielectric relaxation in magnetite single crystals [44–46] and magnetite powder [48] showed a complex dependence of the height of the ϵ'' maximum on crystal orientation and oxygen content. Whereas the dielectric loss in a magnetite powder sample [48] and in SiO_2-coated magnetite nanoparticles [49] is Debye-like, such as in the magnetite film studied here, the dielectric permittivity of magnetite single crystals has the typical features of a relaxor ferroelectric [44–46].

The loss peak frequency f_p follows an Arrhenius law as illustrated in figure 2(b). Using the equation

$$f_p = f_0 \exp\left[-\frac{U}{k_B T}\right] \quad (1)$$

the data were fitted with an activation energy $U = 31$ meV and an attempt frequency $f_0 = 4.5 \times 10^9$ Hz. This is in agreement with permittivity measurements on SiO_2-coated magnetite nanoparticles reporting an activation energy of 40 meV [49]. Assuming a Debye process, $\epsilon'' = \beta(f/f_p)/[1 + (f/f_p)^2]$, the loss component ϵ'' can be calculated using equation (1) and $\beta = 1.8$, see the solid lines in figure 2(a). At low frequencies this yields curves with a width considerably smaller than observed, indicating a relaxation process with a broad distribution of relaxation times and therefore a certain glassiness.

3.3. Magnetoelectric effect of magnetite films

Figure 3(a) shows the real and imaginary parts of the dielectric permittivity of a PLD-fabricated magnetite film measured at 1 kHz in zero magnetic field. Besides the Debye relaxation maximum the loss data in figure 3(a) contain a contribution from the thermally activated conductivity of the sample. The field dependence of the dielectric permittivity was measured in various magnetic fields and is shown in figures 3(b) and (c) for the real and imaginary components, respectively. The magneto-permittivity was defined as $\Delta\epsilon'/\epsilon' = [\epsilon'(H) - \epsilon'(H = 0)]/\epsilon'(H = 0)$ and $\Delta\epsilon''/\epsilon'' = [\epsilon''(H) - \epsilon''(H = 0)]/\epsilon''(H = 0)$. Overall the magnetoelectric effect in the real component ϵ' is small, but shows a pronounced temperature dependence with a maximum close to the Debye peak in ϵ''. The magnetic field dependence of the imaginary component ϵ'' is significantly larger; this might be due to the fact that two processes, i.e. Debye relaxation and electron conduction, contribute to ϵ'' and that the magnetoresistance is considerably larger than the magnetic field dependence of the Debye relaxation.

Figure 4 shows hysteresis curves of the dielectric permittivity for various temperatures and magnetic fields applied in-plane as well as perpendicular to the film. In figures 4(a) and (b) a clear anisotropy in the magnetic field dependence of both permittivity components is seen. At low magnetic fields butterfly-like loops with sharp maxima at the coercive fields were observed; these prove a coupling between

magnetic domain orientation and dielectric permittivity. Whereas the in-plane response appears to be reversible at higher magnetic fields, the perpendicular-to-plane response is strongly hysteretic up to 8 T. Figures 4(c) and (d) show the field dependence of the real part of the permittivity for higher temperatures. Above the temperature of the Debye relaxation maximum at about 23 K the permittivity curves are reversible in magnetic field. In figures 3(b) and (c) the 8 T magneto-permittivity data measured either in constant magnetic field or constant temperature mode are compared. Whereas the data show the same trend as a function of temperature, there are some differences below 10 K for both permittivity components and around 26 K in $\Delta\epsilon''/\epsilon''$. The low temperature differences as well as the strong hysteresis up to 8 T are surprising, since the magnetization should be in technical saturation in such high fields. It is well known, however, that the high field magnetization of magnetite films is significantly influenced by the antiferromagnetic coupling appearing at anti-phase boundaries [50–52]. Therefore the high field hysteretic features might be tentatively related to the presence of anti-phase boundaries that might couple to both magnetization and ferroelectric polarization.

The change in the permittivity is too large to be explained by magnetostriction only, see [53–55] for magnetostriction values. Further, note that in the case of a perpendicular magnetic field the form of the hysteresis curve is uncommon with the appearance of two maxima in one branch of the hysteresis loop.

In comparison, the magnetic field dependence of the permittivity of a magnetite polycrystal was measured at 5 K and various frequencies between 100 kHz and 1 MHz (not shown). Since the magneto-permittivity was frequency-independent, it is not due to a Maxwell–Wagner effect [56].

3.4. Magnetization of magnetite films

The magnetization might yield direct information on the existence of a phase transition, but can also be related to the specific heat. Since the entropy S is related to the magnetization M by the Maxwell relation

$$\left(\frac{\partial S}{\partial H}\right)_T = \mu_0 \left(\frac{\partial M}{\partial T}\right)_H, \tag{2}$$

the field derivative of the heat capacity C_H is related to the magnetization by

$$\left(\frac{\partial C_H}{\partial H}\right)_T = T\mu_0 \left(\frac{\partial^2 M}{\partial T^2}\right)_H. \tag{3}$$

Figure 5 shows the remanent magnetization of the magnetite film as well as $T\partial^2 M/\partial T^2$. The remanence was measured after cooling in various fields from 300 to 5 K and switching the field off at 5 K. The film showed a slope change in the remanent magnetization near 40 K, leading to a gradual rise above the zero level of $T\partial^2 M/\partial T^2$ below about 45 K, see figure 5. The Verwey transition was clearly observed at 115 K. A further anomaly was observed at 11 K, see figure 5. These features might indicate, but are no firm proof of, a thermodynamic transition below 50 K.

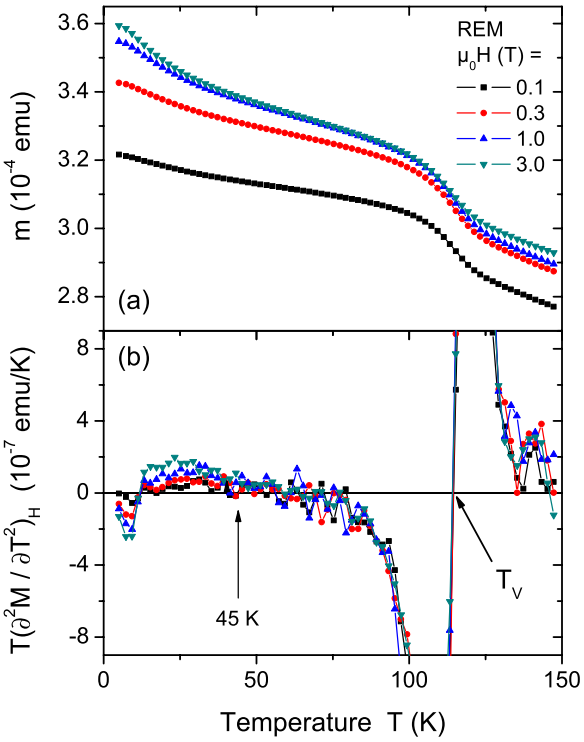

Figure 5. (a) Remanent magnetization of the magnetite film measured after cooling in the magnetic fields specified in the figure. (b) $T\partial^2 M/\partial T^2$ of the remanent magnetization data.

3.5. Specific heat of polycrystalline magnetite

Specific heat data could only be measured on a polycrystalline bulk sample (not shown). Overall the specific heat data were in agreement with published data [46, 57–61]. A sharp λ transition with a transition enthalpy of 982.2 J mol^{-1} was observed at the Verwey transition of 123.4 K. The specific heat below 70 K did not depend on the applied magnetic field, at least not up to 8 T. Above 10 K it was dominated by phonons; in agreement with [46] there was a broad anomaly in C_p/T^3 at about 32 K, indicating glassy behavior. Below 6 K the magnon contribution became important and the specific heat could be fitted to $C_p = aT^{3/2} + bT^3$ with $a = 0.32$ mJ mol^{-1} K$^{-5/2}$ and $b = 0.082$ mJ mol^{-1} K^{-4}, similar to the data of Dixon *et al* [57]. At 10.3 K a sharp peak was observed in the specific heat, reminiscent of the feature reported by Todo and Chikazumi [62]. This feature might indicate a phase transition at 10.3 K and might be related to the anomaly seen at 11 K in $T\partial^2 M/\partial T^2$ of the magnetite film, see figure 5(b).

3.6. AC susceptibility of bulk magnetite

Figure 6(a) shows the real χ' and imaginary (loss) χ'' parts of the susceptibility of the magnetite polycrystal as a function of temperature. In this low-frequency range the susceptibility in magnetite crystals is determined by the domain-wall mobility [63]. In the temperature range between 10 and 300 K the data indicate the presence of three processes: (i) the sharp step in χ' accompanied by the weak dissipation maximum in

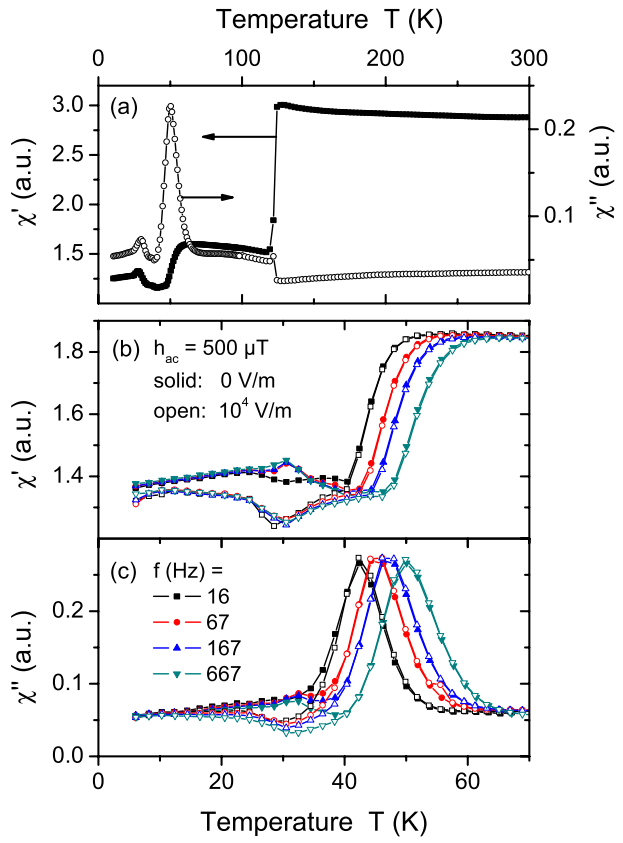

Figure 6. (a) Real and imaginary parts of the ac susceptibility of a magnetite polycrystal in zero dc magnetic field as a function of temperature. Measurement frequency was 667 Hz. (b) Real and (c) imaginary parts of the ac susceptibility of the same sample for various frequencies and applied electric fields of zero and 10^4 V m^{-1}.

χ'' at the Verwey temperature of 123 K is due to a change in the magnetocrystalline anisotropy induced by the structural transition. (ii) A further step in the susceptibility at 52 K is accompanied by a pronounced loss maximum [48, 64, 65]. Since the domain-wall mobility is determined by domain-wall pinning at structural defects as well as by ionic and electronic relaxation within the domain wall, this susceptibility feature indicates a freezing-out of the domain-wall mobility. It occurs at the same temperature as in single crystals [64, 65] and agrees with the onset of a relaxation process with a logarithmic time dependence as detected in magnetic aftereffect measurements [64, 66–69]. (iii) A further weak feature is seen in both susceptibility components at 30 K. Similar features were reported before [70, 71], especially for stoichiometric magnetite samples. This feature might be related to a low temperature relaxation process observed below 30 K in the magnetic aftereffect; the minimum in the real part of the susceptibility corresponds to the relaxation gap between 35 and 50 K observed in magnetic aftereffect measurements [64, 66–68, 70, 71].

Figures 6(b) and (c) present the ac susceptibility of the magnetite polycrystal measured at different frequencies and for electric fields of 0 and 10^4 V m^{-1}. The data very clearly show (i) the frequency dependence of the 50 K anomaly as well as (ii) a magnetoelectric effect in the low temperature regime. This magnetoelectric effect vanishes at a frequency-dependent temperature at the onset of the dynamical process. This indicates that a relaxation mechanism destroys the magnetoelectric effect.

The ac susceptibility loss peak frequency f_p follows the Arrhenius law, equation (1), but with an activation energy $U = 92$ meV and an attempt frequency $f_0 = 1.1 \times 10^{12}$ Hz, see figure 2(b). The constant height of the ac susceptibility loss maximum actually shows that this is a Debye relaxation process. Literature data for a magnetite single crystal yielded an activation energy $U = 40$ meV and an attempt frequency $f_0 = 1.7 \times 10^8$ Hz [65]. The comparison to magnetic aftereffect data [64, 70] is not straightforward, since the aftereffect relaxation plateau extending between 50 K and T_V corresponds to a logarithmic time dependence, indicating a broad distribution of activation energies in the range of 150–350 meV. The ac susceptibility measurements only probe the low energy tail of the distribution which explains the low value of the activation energy. The activation energy will further depend on the domain-wall pinning mechanisms active in the sample; therefore it is not surprising that our polycrystal and the single crystal from [65] have different activation energies.

4. Discussion

The data presented in section 3.6 lead to the following conclusions.

- Magnetite films grown on Nb-doped $SrTiO_3$ substrates by pulsed laser deposition and magnetron sputtering show an electric polarization at low temperatures, see figure 1. The onset temperature of the polarization as well as the low temperature saturation value depend on the preparation technique, i.e. on the real sample structure.
- These magnetite films show a Debye relaxation process in the dielectric permittivity, see figure 2(a). The activation energy of this process is 31 meV, see figure 2(b).
- Further, the magnetite films show magnetoelectric effects in the low temperature regime below the Debye relaxation process with pronounced magnetic field hysteresis, see figures 3 and 4.
- The polycrystals show a Debye relaxation process in the ac susceptibility that indicates freezing of magnetic domain walls, see figure 6. The activation energy of this relaxation process is 92 meV, see figure 2(b).
- Significant magnetoelectric effects were observed in the ac susceptibility below this relaxation process, see figure 6.
- Specific heat measurements on the magnetite polycrystal did not show any evidence for a bulk phase transition in the temperature range between 11 and 70 K.

The data clearly show that magnetoelectric effects occur in both magnetite films and polycrystals. Decisively, these are seen at low temperatures below a frequency-dependent freezing temperature of some relaxation mechanism. Below this freezing temperature the magnetite films are ferroelectric with a sizable electric polarization of the order of 5 μC cm^{-2}.

Thus the films definitely have a polar monoclinic *Cc* structure. Heat capacity measurements do not show a phase transition below the Verwey transition, i.e. the Verwey transition is the thermodynamic transition leading to the multiferroic phase. Since the ferroelectric polarization sets in much below the Verwey temperature, one would classify magnetite as a relaxor ferroelectric [41, 46]. From the literature some clues toward the nature of the relaxation mechanism are obtained:

- Extensive magnetic aftereffect measurements on magnetite samples showed unique relaxation mechanisms that were related to electronic transitions: electron tunneling between Fe^{2+} and Fe^{3+} ions in the temperature range between 5 and 35 K as well as thermally activated electron hopping between Fe^{2+} and Fe^{3+} ions in the temperature range between 50 K and T_V [64, 66–71].
- Studies of the easy-axis switching in magnetite [10, 38–40] revealed thermally activated behavior with an activation energy in the range 25–33 meV.

An analysis and understanding of magnetoelectric and/or multiferroic effects in magnetite does not only have to take into account the crystal symmetry and twin structure, but also oxygen stoichiometry and strain effects. All of these are not well studied and understood in magnetite films. The Verwey temperatures of the magnetite films investigated here are generally around 115 K, i.e. significantly lower than in the bulk. This might be due to non-stoichiometry, the difference in thermal expansion coefficients between film and substrate [72] as well as strain effects, and cannot be used as a direct marker of oxygen content, especially since the film–substrate mismatch with −7% is rather large. In future work the crystallographic domain formation in magnetite films grown under compressive stress will be further studied; these crystallographic data will be correlated with electric polarization values and the characteristics of dielectric and magnetic relaxation processes to obtain further insight into the nature of the relaxor ferroelectric state.

5. Conclusions

The ferroelectric polarization detected in magnetite films [34] and single crystals [27, 30, 46] can be understood in the following scenario. The ferroelectric phase appears at the Verwey transition in the non-centrosymmetric monoclinic *Cc* symmetry. Between 40 K and T_V, however, the electric polarization is suppressed by relaxation processes. These might be either electron tunneling and electron hopping processes [64], glassy polar degrees of freedom [46] or thermally activated structural processes [39]. A comparison of the activation energies of the dielectric Debye process (31 meV (this work), 40 meV [49]), of easy-axis switching (25–33 meV [10, 39]) and of domain-wall motion in single crystals (40 meV [65]) indicates a connection between these phenomena. Since the easy-axis direction is stabilized by the film–substrate strain, it would be easier to observe a ferroelectric polarization in thin films than in bulk. Indeed, the polarization values measured in magnetite films tend to be larger than in single crystals. This scenario naturally explains the close relation between magnetoelectric effects and relaxation processes observed both in the electric and magnetic susceptibility. In contrast to conventional relaxor ferroelectrics [41] in magnetite the relaxor behavior is not driven by chemical heterogeneity, but by dynamical structural disorder.

Acknowledgments

This work was supported by the DFG within the Collaborative Research Center SFB 762 ‘Functionality of Oxide Interfaces’ and by the Spanish MICINN projects MAT2008-06517-C02-01 and CSD2009_00013.

References

[1] Walz F 2002 *J. Phys.: Condens. Matter* **14** R285
[2] Novák P, Štěpánková H, Englich J, Kohout J and Brabers V A M 2000 *Phys. Rev.* B **61** 1256
[3] García J and Subías G 2004 *J. Phys.: Condens. Matter* **16** R145–78
[4] Subías G, García J and Blasco J 2005 *Phys. Rev.* B **71** 155103
[5] Lorenzo J E, Mazzoli C, Jaouen N, Detlefs C, Mannix D, Grenier S, Joly Y and Marin C 2008 *Phys. Rev. Lett.* **101** 226401
[6] Joly Y, Lorenzo J E, Nazarenko E, Hodeau J L, Mannix D and Marin C 2008 *Phys. Rev.* B **78** 134110
[7] Blasco J, García J and Subías G 2011 *Phys. Rev.* B **83** 104105
[8] Anderson P 1956 *Phys. Rev.* **102** 1008
[9] Bickford L R Jr 1953 *Rev. Mod. Phys.* **25** 75
[10] Calhoun B A 1954 *Phys. Rev.* **94** 1577
[11] Hamilton W C 1958 *Phys. Rev.* **110** 1050
[12] Medrano C, Schlenker M, Baruchel J, Espeso J and Miyamoto Y 1999 *Phys. Rev.* B **59** 1185
[13] Wright J P, Attfield J P and Radaelli P G 2001 *Phys. Rev. Lett.* **87** 266401
[14] Wright J P, Attfield J P and Radaelli P G 2002 *Phys. Rev.* B **66** 214422
[15] Zuo J M, Spence J C H and Petuskey W 1990 *Phys. Rev.* B **42** 8451
[16] Leonov I, Yaresko A N, Antonov V N, Korotin M A and Anisimov V I 2004 *Phys. Rev. Lett.* **93** 146404
[17] Jeng H T, Guo G Y and Huang D J 2004 *Phys. Rev. Lett.* **93** 156403
[18] Jeng H T, Guo G Y and Huang D J 2006 *Phys. Rev.* B **74** 195115
[19] Piekarz P, Parlinski K and Oleś A M 2007 *Phys. Rev.* B **76** 165124
[20] Rado G T and Ferrari J M 1975 *Phys. Rev.* B **12** 5166
[21] Rado G T and Ferrari J M 1977 *Phys. Rev.* B **15** 290
[22] Iida S, Mizoguchi M, Umemura S, Yoshida J, Kato K and Yanai K 1979 *J. Appl. Phys.* **50** 7584
[23] Siratori K, Kita E, Kaji G, Tasaki A, Kimura S, Shindo I and Kohn K 1979 *J. Phys. Soc. Japan* **47** 1779
[24] Kita E, Siratori K, Kohn K, Tasaki A, Kimura S and Shindo I 1979 *J. Phys. Soc. Japan* **47** 1788
[25] Kato K and Iida S 1981 *J. Phys. Soc. Japan* **50** 2844
[26] Kato K and Iida S 1982 *J. Phys. Soc. Japan* **51** 1335–6
[27] Kato K, Iida S, Yanai K and Mizushima K 1983 *J. Magn. Magn. Mater.* **31–34** 783–4
[28] Miyamoto Y, Kobayashi M and Chikazumi S 1986 *J. Phys. Soc. Japan* **55** 660–5
[29] Inase T and Miyamoto Y 1987 *J. Phys. Soc. Japan* **56** 3683–8
[30] Miyamoto Y and Chikazumi S 1988 *J. Phys. Soc. Japan* **57** 2040–50

[31] Miyamoto Y and Ishiyama K 1993 *Solid State Commun.* **81** 581–3
[32] Miyamoto Y and Shindo M 1993 *J. Phys. Soc. Japan* **62** 1423–6
[33] Miyamoto Y 1994 *Ferroelectrics* **161** 117–23
[34] Alexe M, Ziese M, Hesse D, Esquinazi P, Yamauchi K, Fukushima T, Picozzi S and Gösele U 2009 *Adv. Mater.* **21** 4452–5
[35] van den Brink J and Khomskii D I 2008 *J. Phys.: Condens. Matter* **20** 434217
[36] Yamauchi K, Fukushima T and Picozzi S 2009 *Phys. Rev.* B **79** 212404
[37] Höhne R, Kleint C A, Pan A V, Krause M K, Ziese M and Esquinazi P 2000 *J. Magn. Magn. Mater.* **211** 271–7
[38] Matsui M, Todo S and Chikazumi S 1977 *J. Phys. Soc. Japan* **43** 47–52
[39] Chlan V, Kouřil K, Štěpánková H, Řezníček R, Štěpánek J, Tabiś W, Król G, Tarnawski Z, Kakol Z and Kozłowski A 2010 *J. Appl. Phys.* **108** 083914
[40] Kakol Z, Król G, Tabiś W, Kołodziej T, Wiśniewski A, Štěpánková H, Chlan V, Kusz J, Tarnawski Z, Kozłowski A and Honig J M 2011 *J. Phys.: Conf. Ser.* **303** 012106
[41] Cross L E 1987 *Ferroelectrics* **76** 241
[42] von Hippel A R 1954 *Dielectrics and Waves* (New York: Wiley)
[43] Catalan G, O'Neill D, Bowman R M and Gregg J M 2000 *Appl. Phys. Lett.* **77** 3078
[44] Kobayashi M, Akishige Y and Sawaguchi E 1986 *J. Phys. Soc. Japan* **55** 4044–52
[45] Kobayashi M, Akishige Y and Sawaguchi E 1988 *J. Phys. Soc. Japan* **57** 3474
[46] Schrettle F, Krohns S, Lunkenheimer P, Brabers V A M and Loidl A 2011 *Phys. Rev.* B **83** 195109
[47] Jonscher A K 1999 *J. Phys. D: Appl. Phys.* **32** R57
[48] Iwauchi K, Kita Y and Koizumi N 1980 *J. Phys. Soc. Japan* **49** 1328
[49] Chang C C, Zhao L and Wu M K 2010 *J. Appl. Phys.* **108** 094105
[50] Margulies D T, Parker F T, Rudee M L, Spada F E, Chapman J N, Aitchison P R and Berkowitz A E 1997 *Phys. Rev. Lett.* **79** 5162–5
[51] Eerenstein W, Palstra T T M, Hibma T and Celotto S 2002 *Phys. Rev.* B **66** 201101(R)
[52] Bataille A M, Ponson L, Gota S, Barbier L, Bonamy D, Gautier-Soyer M, Gatel C and Snoeck E 2006 *Phys. Rev.* B **74** 155438
[53] Bickford L R Jr, Pappis J and Stull J L 1955 *Phys. Rev.* **99** 1210
[54] Arai K I, Ohmori K, Tsuya N and Iida S 1976 *Phys. Status Solidi* a **34** 325
[55] Belov K P, Goryaga A, Sheremet'ev V and Naumova O 1985 *JETP Lett.* **42** 117
Belov K P, Goryaga A, Sheremet'ev V and Naumova O 1985 *Pis. Zh. Eksp. Teor. Fiz.* **42** 97–9
[56] Catalan G 2006 *Appl. Phys. Lett.* **88** 102902
[57] Dixon M, Hoare F E and Holden T M 1965 *Phys. Lett.* **14** 184
[58] Westrum E F Jr and Grønvold F 1969 *J. Chem. Thermodyn.* **1** 543–57
[59] Shepherd J P, Koenitzer J W, Aragón R, Sandberg C J and Honig J M 1985 *Phys. Rev.* B **31** 1107
[60] Shepherd J P, Koenitzer J W, Aragón R, Spałek J and Honig J M 1991 *Phys. Rev.* B **43** 8461
[61] Takai S, Akishige Y, Kawaji H, Atake T and Sawaguchi E 1994 *J. Chem. Thermodyn.* **26** 1259–66
[62] Todo S and Chikazumi S 1977 *J. Phys. Soc. Japan* **43** 1091
[63] Kronmüller H 1968 *Nachwirkung in Ferromagnetika* (Heidelberg: Springer)
[64] Walz F and Kronmüller H 1994 *Phys. Status Solidi* b **181** 485
[65] Skumryev V, Blythe H J, Cullen J and Coey J M D 1999 *J. Magn. Magn. Mater.* **196/197** 515–7
[66] Kronmüller H and Walz F 1980 *Phil. Mag.* B **42** 433–52
[67] Walz F, Weidner M and Kronmüller H 1980 *Phys. Status Solidi* a **59** 171
[68] Walz F, Deusch H and Kronmüller H 1979 *Phys. Status Solidi* a **53** 519
[69] Kronmüller H 1977 *J. Magn. Magn. Mater.* **4** 280–6
[70] Walz F, Brabers V A M, Chikazumi S, Kronmüller H and Rigo M O 1982 *Phys. Status Solidi* b **110** 471
[71] Walz F and Kronmüller H 1990 *Phys. Status Solidi* b **160** 661
[72] van der Zaag P J, Fontijn W F J, Gaspard P, Wolf R M, Brabers V A M, van de Veerdonk R J M and van der Heijden P A A 1996 *J. Appl. Phys.* **79** 5936